



**QUEEN'S  
UNIVERSITY  
BELFAST**

## Comprehensive analysis of mouse retinal mononuclear phagocytes

Lückoff, A., Scholz, R., Sennlaub, F., Xu, H., & Langmann, T. (2017). Comprehensive analysis of mouse retinal mononuclear phagocytes. DOI: 10.1038/nprot.2017.032

**Published in:**  
Nature Protocols

**Document Version:**  
Peer reviewed version

**Queen's University Belfast - Research Portal:**  
[Link to publication record in Queen's University Belfast Research Portal](#)

**Publisher rights**

© 2017 Macmillan Publishers Limited, part of Springer Nature. All rights reserved. This work is made available online in accordance with the publisher's policies. Please refer to any applicable terms of use of the publisher.

**General rights**

Copyright for the publications made accessible via the Queen's University Belfast Research Portal is retained by the author(s) and / or other copyright owners and it is a condition of accessing these publications that users recognise and abide by the legal requirements associated with these rights.

**Take down policy**

The Research Portal is Queen's institutional repository that provides access to Queen's research output. Every effort has been made to ensure that content in the Research Portal does not infringe any person's rights, or applicable UK laws. If you discover content in the Research Portal that you believe breaches copyright or violates any law, please contact [openaccess@qub.ac.uk](mailto:openaccess@qub.ac.uk).

## **Comprehensive analysis of mouse retinal mononuclear phagocytes**

Anika Lückoff<sup>1\*</sup>, Rebecca Scholz<sup>1\*</sup>, Florian Sennlaub<sup>2</sup>, Heping Xu<sup>3</sup> & Thomas Langmann<sup>1</sup>

<sup>1</sup>Laboratory for Experimental Immunology of the Eye, Department of Ophthalmology, University of Cologne, Germany.

<sup>2</sup>Institut de la Vision, Sorbonne Universités, UPMC Univ Paris 06, INSERM, CNRS, Paris, France.

<sup>3</sup>Centre for Experimental Medicine, School of Medicine, Dentistry & Biomedical Sciences, Queen's University Belfast, UK.C

\*These authors contributed equally

Correspondence should be addressed to T.L. ([thomas.langmann@uk-koeln.de](mailto:thomas.langmann@uk-koeln.de))

## **ABSTRACT**

The innate immune system is activated in a number of degenerative and inflammatory retinal disorders such as age-related macular degeneration (AMD). Retinal microglia, choroidal macrophages, and recruited monocytes, collectively termed 'retinal mononuclear phagocytes', are critical determinants of ocular disease outcome. Many publications have described the presence of these cells in mouse models for retinal disease; however, only limited aspects of their behavior have been uncovered, and these have only been uncovered using a single detection method. The workflow presented here describes a comprehensive analysis strategy that allows characterization of retinal mononuclear phagocytes in vivo and in situ. We present standardized working steps for scanning laser ophthalmoscopy of microglia from MacGreen reporter mice (mice expressing the macrophage colony-stimulating factor receptor GFP transgene throughout the mononuclear phagocyte system), quantitative analysis of Iba1-stained retinal sections and flat mounts, CD11b-based retinal flow cytometry, and qRT-PCR analysis of key microglia markers. The protocol can be completed within 3 d, and we present data from retinas treated with laser-induced choroidal neovascularization (CNCNV), bright white-light exposure, and Fam161a-associated inherited retinal degeneration. The assays can be applied to any of the existing mouse models for retinal disorders and may be valuable for documenting immune responses in studies for immunomodulatory therapies.

## INTRODUCTION

Retinal glial cells are separated into macroglia and microglia. The two macroglial cell populations in the retina are Müller cells and astrocytes. Müller cells are essential for retinal physiology including neurotransmitter and metabolite homeostasis and support the blood-retinal barrier<sup>1</sup>. Astrocytes are located to the nerve fibre layer where they shield ganglion cell axons and envelop blood vessels, thereby also contributing to the inner blood-retinal barrier<sup>2</sup>. Upon retinal damage, both cell types typically respond with reactive gliosis<sup>2</sup>. Microglia, the third glial cell type of the retina, belongs to the resident tissue macrophage population of the central nervous system<sup>3</sup>.

In the healthy adult retina, microglia show a distinct ramified morphology and are exclusively located in the inner and outer plexiform layers<sup>4</sup>. Their somata are relatively static under physiological conditions and a regularly spaced cellular network spans the whole inner retina<sup>5</sup>. From these strategic positions microglia constantly scan the retina with their long protrusions, sensing disturbance in tissue homeostasis<sup>6</sup>. They can rapidly respond to retinal insults often associated with cellular migration to the sites of damage<sup>7</sup>. Concomitantly, the cells retract their protrusions and transform into amoeboid phagocytes that can produce a variety of neurotoxic inflammatory mediators including reactive oxygen species and cytokines<sup>8</sup>. Reactive microglia clear dying neurons but can also damage and phagocytose whole living photoreceptors in the diseased developing retina<sup>9,10</sup>. Under specific conditions of retinal lipid accumulation, intraretinal or subretinal microglia appear as lipid-bloated cell aggregates<sup>11,12</sup>.

In addition to resident microglia, the mononuclear phagocyte population in the retinal area also includes local macrophages of the vasculature, the ciliary body, and choroid as well as infiltrating macrophages that differentiate from blood monocytes. The mononuclear phagocytes that infiltrate the subretinal space in conditions when the blood retinal barriers are compromised can be distinguished from resident microglia by different technological approaches. Studies that generated bone marrow chimeras with EGFP-transgenic mice and performed subsequent flow cytometry showed that perivascular macrophages expressed less F4/80, CD45, and Iba-1 compared with parenchymal microglia<sup>13</sup>. However, the use of bone marrow transplantation to generate GFP+ leukocyte chimeras is problematic as it necessitates total body irradiation which may alter microglia function and cranial sparing resulting in incomplete bone marrow engraftment. To better evaluate the extent of inflammatory monocytes in subretinal mononuclear phagocyte accumulation, we previously used a simpler method<sup>14</sup>. We permanently marked the circulating monocytes with repeated EdU injections, a traceable nucleotide that is integrated in the DNA of dividing cells, prior to and during light-induced subretinal inflammation in Cx3cr1<sup>-/-</sup> mice. Three daily intraperitoneal injections were sufficient and necessary to mark the majority of the short lived circulating monocytes. The

number of subretinal EdU+ cells can then be compared in mice with and without clodronate-liposome-induced monocyte depletion. Local EdU administration failed to mark subretinal cells, suggesting that ocular proliferation does not play a significant role in the light-induced accumulation of subretinal macrophages<sup>14</sup>. This technique can only be used for short-term experiments and is not adapted for the evaluation of chronic inflammation. To evaluate the participation of monocyte-derived cells versus microglia in a more definite and less invasive way, fate-mapping experiments with Cx3Cr1<sup>CreER</sup> mice and R26-YFP reporter mice were reported recently<sup>15,16</sup>. Tamoxifen treatment of the resulting Cx3Cr1<sup>CreER</sup> : R26-stop-YFP mice induces YFP expression in all Cx3cr1-expressing cells. Resident phagocytes including microglia express Cx3cr1 most strongly, along with a subset of monocytes. Due to their faster turnover rate, labeled monocytes are replaced by non-labeled cells once tamoxifen dissipates. In contrast, longer-lived microglia and macrophages retain the fluorescent label and consequently show YFP expression. Applying multicolor flow cytometry on retinas of this model, O'Koren et al. have shown that retinal microglia have a unique cell surface marker profile with low expression of CD45, CD11c, F4/80, and I-A/I-Elo that is also maintained in a light challenge paradigm<sup>16</sup>. The intravenous administration of fluorochrome-conjugated anti-CD45 antibody then allowed exclusion of CD45<sup>+</sup> circulating cells from retinal mononuclear phagocyte analyses<sup>16</sup>. These FACS-based methods could differentiate resident from infiltrating mononuclear phagocytes in whole eye, or in retinal single cell suspensions. Similarly, we have recently shown that resident mononuclear phagocytes play a key role in the mouse model of laser-induced choroidal neovascularization (CNV) that mimics the exudative form of age-related macular degeneration (AMD)<sup>15</sup>.

### **Development of the protocol**

Phagocytic murine retinal microglia have been traced by retro-grade labeling of ganglion cells with different dyes<sup>17</sup>, but more common now is *in vivo* imaging with GFP-expressing transgenic animals<sup>18-21</sup> and/or immunostaining with the marker ionized calcium binding adapter molecule 1 (Iba1)<sup>22</sup>. The retinal fundus is optimal for non-invasive imaging and GFP-labeled or autofluorescent phagocytes can be visualized with a confocal scanning laser ophthalmoscope in the blue auto-fluorescence mode. This procedure is especially useful in conditions where GFP+ microglia accumulate at focal lesion areas around atrophic areas<sup>23</sup> or close to experimental laser spots<sup>18,21</sup>. Microglia can be directly imaged when they contain auto fluorescent endogenous lipids due to lipid storage disease<sup>11</sup> or when they have ingested large amounts of lipofuscin granules related to retinal aging processes<sup>24</sup>.

We have previously compared F4/80 and Iba1 to visualize retinal microglia in retinal sections and flat mounts of retinoschisin-deficient mice, a model for human X-linked retinoschisis, and found that Iba1 is superior to F4/80 in both types of *in situ* methods<sup>25</sup>. In fact, most recent *in situ* analyses of ramified and reactive retinal microglia rely on Iba1 staining<sup>26-30</sup> as the marker allows consistent and reliable staining of microglia somata and their processes in a broad spectrum of different activation phenotypes<sup>31-33</sup>. In general, a combined *in situ* analysis of retinal microglia using sections and flat mounts as presented in our protocol is recommended. This allows the counting of ramified and amoeboid mononuclear phagocytes and characterization of their morphology using a quantitative grid cross method<sup>32,34</sup>.

In our previous work, we also have performed retinal microglia analysis using flow cytometry and gene expression profiling. We have learned that Iba1 is not optimal for FACS as it requires a longer intracellular staining procedure and leads to more nonspecific signals. However, CD11b (OX42), a broadly expressed integrin marker of mononuclear phagocytes is suitable to determine relative numbers in either total retinal cell homogenates<sup>32,35</sup> or pre-sorted phagocyte populations<sup>36</sup>.

Gene expression analyses for microglia markers either in total retinal RNA or in sorted cells is a very useful tool to determine their activation phenotype. We have previously characterized the macrophage/microglia WAP domain protein (AMWAP) as a regulator of pro-inflammatory response<sup>37,38</sup>. AMWAP transcription is rapidly induced in microglia from different retinal disease mouse models, including inherited photoreceptor dystrophies and different light challenge paradigms<sup>7,32,33,39</sup>. Another good marker to detect microglia reactivity is CC-chemokine ligand 2 (CCL2, alias monocyte chemoattractant protein 1, MCP-1), which has a key role in pro-inflammatory mononuclear phagocyte chemotaxis and migration in the retina<sup>14,40</sup>.

## Overview of the procedure

The workflow of the analysis is illustrated in **Figure 1** and contains three main steps: a) *in vivo* imaging via OCT analysis, b) histological and c) molecular analysis of retinal mononuclear phagocytes. The histological analysis comprises stainings of retinal cryo sections and flat mounts to analyze the cellular distribution and morphology from two different perspectives. Furthermore, flow cytometry and gene expression profiling help to describe the activation status of mononuclear phagocytes and their contribution to disease progression. The characterization strategy presented here includes common laboratory methods such as

fluorescence microscopy, flow cytometry and qRT-PCR but requires basic understanding of retinal anatomy and immunology.

### **Applications of this method**

We have recently applied main parts of the protocol to fully characterize the protective role of mononuclear phagocyte interferon- $\beta$  signaling in the AMD-related mouse model of laser-induced CNV<sup>15</sup>. Using conventional interferon- $\alpha/\beta$ -receptor knockout mice (IFNAR1<sup>-/-</sup>)<sup>41</sup> and Cx3cr1<sup>CreER</sup>:Ifnar1<sup>fl/fl</sup><sup>15</sup> animals that allowed the tamoxifen-induced conditional depletion of Ifnar in resident mononuclear phagocytes only showed that interferon signaling in resident cells and not inflammatory monocytes play a key role in choroidal neovascularization in this setting. This protocol described here is now routinely established in the authors' laboratories and can be principally applied to any project related to retinal disease that involves mononuclear phagocyte reactivity. Such models of ocular disease include all genetic mouse lines for retinal dystrophies and experimental models for uveitis, glaucoma, diabetic retinopathy, retinopathy of prematurity, AMD, and many others<sup>42-48</sup>.

### **Comparison with other methods and limitations of the protocol**

The very few published protocols to specifically analyze retinal mononuclear phagocytes are limited to individual aspects related to their functional diversity. The *in vivo* responses of phagocytes has been documented in laser injury of the fundus using confocal scanning laser ophthalmoscope<sup>18</sup> and *ex vivo* isolation of microglia and calcium imaging has been used to characterize their phagocytic phenotype<sup>49</sup>. Many more studies used marker staining in retinal sections and to a lesser extent flat mounts to describe the morphology and location of retinal microglia<sup>7,50</sup>.

The general protocol presented here involves a complementary and step-wise procedure to cover as many important aspects of retinal mononuclear phagocyte biology as possible (**Fig. 1**). The first step is imaging for *in vivo* investigation of retinal microglia and infiltrating immune cells in the healthy and diseased retina. The major advantage is that the technique is non-invasive, which allows retinal phagocytes to be studied in living animals at repeated time points such as at different stages of disease. The disadvantage is that the technique can only be used in animals in which myeloid cells are fluorescein-tagged either by genetic engineering or *in vivo* labeling/staining. Moreover, the resolution of *in vivo* imaging is relatively low compared to *in situ* confocal microscopy. The next step is histology to detect microglia in retinal sections

and flat mounts using immunostaining with the marker Iba1. The analysis of sections is especially useful to describe the relative location of cells within the retinal layers and to determine the number of migrating cells in a semi-quantitative manner. A drawback is that the horizontal spacing and network of resident cells cannot be visualized properly. To overcome this limitation, the analysis of corresponding flat mounts, either from the second eye or from other animals in the same experimental group is recommended. Flat mount staining of the retina and the RPE/choroid with Iba1 allows to describe the relative horizontal position of microglia within the regularly spaced network, their accumulation in focal lesion areas and exact morphological description using a quantitative grid cross method. However, very severe or late stage degenerative retinal pathologies may limit flat mount analyses due to tissue atrophy. The next block in our analysis pipeline is based on flow cytometry and gene expression profiling as molecular methods. The advantage of FACS is that quantitative single cell protein expression data can be obtained. Here, we describe the use of CD11b as an exemplary marker that works well to detect most mononuclear phagocytes in the retina. In a slightly adapted protocol, multiple antibody markers can be used to differentiate resident phagocytes from infiltrating monocytes<sup>16,35</sup>. Finally, we present gene expression profiling of total retinal transcripts for AMWAP and CCL2, two markers related to microglia activation. Clearly, the limitation here is that only two transcripts are quantified. However, the expression of both markers mirrors mononuclear phagocyte activation in a broad range of retinal disease models<sup>7</sup>. Given the relative small amount of RNA from retinal samples it is advised to focus on selected marker genes. A potential perspective of our protocol is to perform gene expression profiling in flow cytometry or magnetic-activated cell (MACS, Miltenyi Biotec) sorted mononuclear phagocyte populations.

## **Experimental design**

**Mouse models and *in vivo* imaging.** We applied the laser-CNV model<sup>44</sup> to C57BL/6J mice and transgenic MacGreen<sup>19</sup> animals, where a macrophage colony-stimulating factor receptor GFP transgene is expressed throughout the mononuclear phagocyte system of the mouse<sup>19</sup>. Adult 6-8 week old mice are most appropriate for laser-CNV induction. As the mouse strain seems to influence CNV severity, appropriate back-crossing and littermate controls are recommended<sup>51</sup>. Subsequent analyses of infrared images and blue auto-fluorescence images from the same animal allows correlation of the impact of the laser lesions with the location and recruitment of mononuclear phagocytes (**Fig. 2**).

**Cross sections.** To reproduce consistent and reliable immunohistochemical stainings, we use cryo embedded tissue. Using this protocol, the embedded tissue is less dehydrated and the



antigens are better conserved compared to paraffin embedded tissue. This has a major impact on the staining quality and facilitates to display the distinct cell morphology (**Fig. 3**).

**Flat mounts.** In this protocol we describe the flat mount analysis of the inner retina. This method allows the characterization of resident retinal microglia distribution and morphology. Depending on the disease model, RPE/choroidal flat mounts can allow quantification of cell migration and cell accumulation in the subretinal space. In the laser-CNV model, reactive mononuclear phagocytes are a heterogeneous cell population consisting of microglia, choroidal macrophages and invading blood derived cells (**Fig. 4**).

**Quantification of microglia morphology.** Counting of ramified versus round-shaped amoeboid cells in images of mononuclear phagocyte stainings provides a rapid but rough estimation of microglia morphology. As this method is subjective it can be difficult to accurately distinguish single cells from each other and to judge their activation status. We therefore highly recommend combining this method with a complementary quantification method. In our hands, the grid cross analysis is the best tool to describe and compare ramified versus amoeboid cell shapes in different experimental groups (**Fig. 4**)<sup>15,34</sup>.

**Flow cytometry.** To specifically detect mononuclear phagocytes in the retina we stained dissociated tissue with fluorescently-labeled anti-CD11b+ antibody (**Fig. 5**). Flow cytometry enables to accurately quantify the percentage of mononuclear phagocytes in the retina in a relatively short time. This allows comparing their abundance in a broad spectrum of disease conditions. We have established a very robust protocol using the surface integrin marker CD11b and found that staining of intracellular markers is in most cases not recommended. Such protocols for staining of intracellular markers require a further permeabilization step, which increases the duration of the assay, and often leads to increased nonspecific binding. For specific questions such as fate mapping of individual mononuclear cell populations, simultaneous expression of several cell surface markers can be determined by multi-color flow cytometry<sup>16</sup>. The gating strategy and the required staining controls are provided in **Supplementary Fig. 1**.

**Gene expression.** Gene expression analysis presented in this protocol aims at measuring transcript levels of two microglia marker genes, AMWAP<sup>38</sup> and CCL2<sup>52</sup>, in the complete retina. In three different disease models, namely genetic deletion of the Retinitis Pigmentosa Protein Fam161a<sup>39</sup>, in the laser-CNV model and in the light damage paradigm, these two markers reliably detect microglia reactivity (**Fig. 6**). Depending on the project, expression profiles reflecting general retinal inflammation or markers influenced by oxidative stress and constituents of the complement system could be determined. Since the amount of total RNA pooled from two retinas of the same animal is relatively high, a broad spectrum of additional

markers and reference genes could be analyzed depending on the specific research aims. Marker profiling of FACS-isolated cells is also possible and the use of a CD11b-based sorting method has been successfully demonstrated for CX3CR1-GFP expressing microglia<sup>53</sup>. However, because of limited sample quantity, quantification of expression data may be more prone to error.

## MATERIALS

### REAGENTS

#### General reagents

- Mice on C57BL/6J or BALB/c background. **! CAUTION** All animal experiments must comply with national laws and institutional regulations. In our experiments, ARVO (Association for Research in Vision and Ophthalmology) guidelines were followed.
- Bovine Serum Albumin (BSA) (Sigma-Aldrich, cat. no. A9418)
- 1.5 ml vials (Sarstedt, cat. no. 72.690)
- 2 ml vials (Sarstedt, cat. no. 72.689)
- 15 ml Falcon tube (Sarstedt, cat. no. 62.554.502)
- 50 ml Falcon tube (Sarstedt, cat. no. 62.554.254)
- Gloves (Braun, 9205926)
- 96-well plate (Sarstedt, cat. no. 82.1581.001)
- 30 µl pipette tips (Matrix, cat. no. 7432)
- Pipette tips (Sarstedt, cat. no. 70.760.002)
- Phosphate buffered saline (PBS) (Amaresco, cat. no. E404)
- β-Mercaptoethanol (Sigma-Aldrich, cat. no. M-7154)
- Transfer pipette 3.5 ml (Sarstedt, cat.no. 86.1173)

#### *In vivo* Imaging

- 0.9% (w/v) NaCl (Fresenius Kabi, cat. no. 06605514)
- Ketavet (ketaminehydrochloride) (Pfizer Animal Health)
- Rompun (Xylazinehydrochlorid) (Bayer HealthCare)
- 1 ml syringe (BD Plastipak™)
- 30G needle (BD Microlance™)
- Phenylephrin 2.5% (w/v)
- Tropicamid 0.5% (w/v)
- Hylo-Vision® Gel sine (Omni Vision GmbH)

#### Immunohistochemistry

- anti-Iba1 antibody (Wako, cat. no. 01-1074) ▲ **CRITICAL** Store in aliquots to avoid frequent thawing.
- Alexa Fluor 488 antibody (goat anti-rabbit) (Thermo Fisher, cat. no. A-11008)
- Cover glasses 18x18mm (Th.Geyer GmbH)
- Cryomoldes (Tissue-TEK®, cat. no. 4557)
- 4',6-Diamidin-2-phenylindol (DAPI) (Invitrogen, cat. no. D1306)
- Fluorescent Mounting Medium (Dako, cat. no. 53023)
- Microtome Blades C35 TYPE (Feather)
- Pink PAP Pen (Zytomed Systems, cat. no. ZUC064)
- Paraformaldehyde (PFA) (Sigma-Aldrich, cat. no. P6148) ! **CAUTION** PFA is toxic and a potential carcinogen. It should be handled with care and discarded as hazardous waste.
- Powdered milk (Roth, cat. no. T145.3)
- Sodium azide (NaN<sub>3</sub>) (Roth, cat. no. 4221) ! **CAUTION** NaN<sub>3</sub> is highly toxic and very dangerous for the environment. It should be handled with care and discarded as hazardous waste.
- Sucrose (Merck, cat. no. 1.07651)
- Superfrost® PLUS microscope slide (Fisher Scientific, cat. no. 12-550-15)
- Triton X-100 (Sigma-Aldrich, cat. no. X100)
- Tween-20 (Sigma-Aldrich, cat. no. P1379)
- Tissue-Tek O.C.T. compound (Hartenstein)

### Flow cytometry

- CD11b-APC antibody, Reactivity: mouse, human, Clone: M1/70.15.11.5 (isotype: rat IgG2b). (MACS Miltenyi Biotec, cat. no. 130-098-088) ▲ **CRITICAL** Store at 2-8 °C and protect from light. Contains stabilizer and 0.05% (w/v) sodium azide ! **CAUTION** sodium azide is highly toxic and very dangerous for the environment. It should be handled with care and discarded as hazardous waste.
- Rat IgG2b isotype control antibody – APC, clone ES26-5E12.4 is specific for KLH (keyhole limpet hemocyanin). This protein is not expressed on mammalian cells. (MACS Miltenyi Biotec, cat. no. APC 130-102-664) ▲ **CRITICAL** Store at 2-8 °C and protect from light. Contains stabilizer and 0.05% (w/v) sodium azide. Do not freeze. The expiration date is given by the manufacturer and usually indicated on the vial label. ! **CAUTION** sodium azide is highly toxic and very dangerous for the environment. It should be handled with care and discarded as hazardous waste.
- FcR Blocking Reagent, mouse (MACS Miltenyi Biotec, cat. no. 130-092-575) ▲ **CRITICAL** Store at 2-8 °C and protect from light. Contains stabilizer and 0.05% (w/v) sodium azide. Do not freeze. The expiration date is given by the manufacturer and usually indicated on the vial label. ! **CAUTION** sodium azide is highly toxic and very dangerous for the environment. It should be handled with care and discarded as hazardous waste.
- DPBS Dulbecco's Phosphate Buffered Saline with calcium and magnesium (Bio Whittaker, Lonza, cat. no. BE17-513F)

- Ethylenediaminetetraacetic acid (EDTA) (Sigma-Aldrich, cat. no. E9884)
  - FACS buffer: PBS, 2mM EDTA, 0.5% (w/v) BSA, pH 7,2
  - Viobility 405/452 <sup>TM</sup> Fixable Dye (MACS Miltenyi Biotec, cat. no. 130-110-205) **CRITICAL** Store dry and protect from light. Viobility 405/452 <sup>TM</sup> Fixable Dye can be excited by the violet 405 nm laser and has a peak excitation of 450 nm, that can be detected using a 450/50 band pass filter (equivalent to Pacific Blue®)
  - FluoroFix Buffer (Biolegend, cat. no. 422101, storage at at 2-8 °C) **! CAUTION** The fixation buffer contains paraformaldehyde, which is toxic and mutagenic.
  - 1.5ml micro tube (Sarstedt, cat. no. 72.690.001)
  - β-Mercaptoethanol (Gibco 50mM, cat.no.31350010) **! CAUTION** β-Mercaptoethanol is toxic and dangerous for the environment. It should be handled with care and discarded as hazardous waste.
  - Neural Tissue Dissociation Kit- Postnatal neurons, (MACS Miltenyi Biotec, cat. no. 130-094-802, storage at 2-8 °C, protect from light)
  - 5ml Polysterene Round – Bottom Tube with cell strainer (BD Falcon, 12x75mm, style 2262790, cat. No. 352235)
- ▲ **CRITICAL** All reagents and equipment may be substituted with alternatives from other manufacturers.

### Gene expression

- Adhesive qPCR seal (4titude, cat. no. 4ti-0560)
- dNTP Mix, 10 mM each (Thermo Scientific, cat. no. R0132)
- Dual-labeled probe (Roche Universal Probe Library, Roche)
- Ethanol (AppliChem, cat. no. A3678)
- FastStart Universal Probe Master (Roche, cat. no. 14943600)
- Filter tips Biophere® (Sarstedt, cat. no. 70.762.217 – 211)
- NucleoSpin® RNA Mini Kit (Macherey-Nagel, cat. no. 740955)
- PCR stripes (Biozym, cat. no. 711030)
- 384 PCR plate FrameStar® (4titude, cat. no. 4ti-0384/c)
- RevertAid<sup>TM</sup> RT Kit (Thermo Scientific, cat. no. K1691)
- RevertAid<sup>TM</sup> M-MuLV (Thermo Scientific, cat. no. EPO441)
- TaqMan Gene Expression Master Mix (Invitrogen Life Technologies)
- Taq Polymerase (Qiagen, cat. no. 105476)

▲ **CRITICAL** All reagents and equipment may be substituted with alternatives from other manufacturers.

### EQUIPMENT

- 7900 HT Fast Real-Time PCR System (AB Applied Biosystems)
- Adventurer™ Pro balance (Ohaus®)
- ApoTome.2 (Zeiss)
- AxioCam ICc 1 camera (Zeiss)
- AxioCam MRm camera (Zeiss)
- Centrifuge 5415 R (Eppendorf)
- Centrifuge Mini Star (VWR International)
- Cryostat CM3050 (Leica)
- Explorer® Ex 124 balance (Ohaus®)
- Imager.M2 microscop (Zeiss)
- Heraeus Labofuge 400 R (Thermo Scientific)
- HRA+OCT Spectralis (Heidelberg Engineering)
- NanoDrop 2000 Spectrophotometer (Thermo Scientific)
- See-saw rocker SSL4 (Stuart®)
- Stainless steel bead, 5 mm diameter (Qiagen, cat. no. 69989)
- TissueLyser LT (Qiagen, cat. no. 69980)
- Vortex-genie® (Scientific Industries™)
- BD FACS Canto II
- Thermomixer compact (Eppendorf)

## SOFTWARE

- GraphPad PRISM 6 (GraphPad Software, Inc.)
- Spectralis HRA+OCT Software (Heidelberg Engineering)
- ImageJ (Wayne Rasband, NIH)
- Office Suite (Microsoft Corporation)
- RQ Manager 1.2.1 (Applied Biosystems)
- SDS 2.3 (Applied Biosystems)
- Flowjo software (Treestar Inc., Ashland, OR, USA)

## REAGENT SETUP

- ***In vivo Imaging: Anesthesia solution*** Mix 3.2 ml 0.9% (w/v) NaCl with 0.6 ml Ketavet and 0.3 ml Rompun 2% (w/v). To anesthetize the mouse, inject 0.1 ml anesthesia solution per 20 g body weight. Use a 30G needle for intraperitoneal injection.  
▲ **CRITICAL** Prepare this solution fresh each time.
- ***Immunohistochemistry: 4% (w/v) PFA*** Mix 4 mg paraformaldehyde in 100 ml 1x PBS. This solution can be stored at 4°C, protected from light for up to 6 months. **! CAUTION** PFA is toxic and a potential carcinogen. It should be handled with care and discarded as hazardous waste.

- **Immunohistochemistry: 30% Sucrose** Mix 30 mg sucrose in 100 ml aqua dest. This solution can be stored at 4°C.
- **Immunohistochemistry: Antibody solution** Mix 2 % (w/v) BSA, 0.2 % (w/v) NaN<sub>3</sub>, 0.1 % (v/v) Triton X-100 in 1x PBS. This solution can be stored at 4°C up to one year. **! CAUTION** NaN<sub>3</sub> is highly toxic. It should be handled with care and discarded as hazardous waste.
- **Immunohistochemistry: Blocking solution (BLOTTO)** Mix 1 % (w/v) milk, 0.1 % (v/v) Tween 20 in 1xPBS.  
▲ **CRITICAL** Prepare this solution fresh each time.
- **Immunohistochemistry: DAPI solution** 0.1 µg in 1x PBS. This solution can be stored at 4°C, protected from light for up to one month.
- **Immunohistochemistry: Permeabilization buffer** Mix 5 % (v/v) Triton X-100, 5 % (v/v) Tween 20 in 1x PBS.  
▲ **CRITICAL** Prepare this solution fresh each time.

### Flow cytometry

- **Flow Cytometry: FACS buffer:** Prepare a solution containing PBS, 2mM EDTA, 0.5% (w/v) bovine serum albumin (BSA), pH 7.2. This solution can be stored at 4°C up to one month. ▲ **CRITICAL** Buffers containing Ca<sup>2+</sup> or Mg<sup>2+</sup> are not recommended for surface antigen staining and flow cytometry.

### Gene expression

- **Gene expression: qRT-PCR reaction mixture** (10 µl per reaction) Mix 50ng cDNA, 1x TaqMan Gene Expression Master Mix (Invitrogen Life Technologies), 200 nM primers and 0.25 µl dual-labeled probe (Roche Universal Probe Library, Roche). ▲ **CRITICAL STEP** Prepare this solution fresh each time.

## EQUIPMENT SETUP

- HRA+OCT Spectralis (Heidelberg Engineering). ▲ **CRITICAL** To obtain a wide field view of the fundus use a 55° wide-angle lens (SPECTRALIS, No. 18868). GFP tagged microglia can also be imaged by the Micron IV system (Phoenix Research Labs), although the images are not as sharp due to lack of confocal functions.
- BD FACS Canto II, if you use the fixable viability dye eFluor® 450 (e-Bioscience), you need a flow cytometer with a violet laser.

## PROCEDURE

### In vivo retinal imaging •TIMING 15 min per mouse

1 | Anesthetize the mice by intraperitoneal injection with anesthesia solution at an appropriate dose (0.1 ml anesthesia solution/ 20 g body weight). Anesthesia is effective for 30-40 minutes.

▲ **CRITICAL STEP** This step must be performed by licensed and qualified individuals according to the animal welfare guidelines of the institutions.

▲ **CRITICAL STEP** After 15-20 min the lens may get dull, so the funduscopy analyses should start immediately after anesthesia.

#### ? TROUBLESHOOTING

2 | Dilate the pupils of the mouse using 2.5% (w/v) Phenylephrin and 0.5% (w/v) Tropicamid.

▲ **CRITICAL STEP** Wait for 5 min until the pupils are completely dilated. This is necessary to image the complete fundus.

#### ? TROUBLESHOOTING

3 | Analyze the location of laser spots and the distribution of mononuclear phagocytes by infrared images (IR) and blue auto-fluorescence (BAF) with the HRA+OCT Spectralis machine.

▲ **CRITICAL STEP** To prevent the eye surface from desiccating constantly moisten the eyes with Hylo-Vision® Gel sine. Dry eye surface influences the light beam and decreases the quality of funduscopy images. Remove the liquid drop before funduscopy, because it also decreases the quality of the funduscopy images.

▲ **CRITICAL STEP** To obtain high quality *in vivo* images make sure that the eye is positioned straight in front of the Spectralis lens.

#### ? TROUBLESHOOTING

4 | Start with infrared images (IR) where you can localize a laser spot (**Fig. 2a, c**)

#### ? TROUBLESHOOTING

5 | Switch to blue auto-fluorescence (BAF) to analyze the distribution of mononuclear phagocytes e.g. in MacGreen mice (**Fig. 2b, d**).

▲ **CRITICAL STEP** The amount of auto-fluorescent signal can vary in different reporter mouse models.

#### ? TROUBLESHOOTING

### Immunohistochemistry •TIMING 4.5 h

6 | Prepare 4% (w/v) PFA

7 | Prepare Permeabilization buffer

8 | Prepare BLOTTO

9 | Prepare antibody solution

10 | Dilute primary antibody in antibody solution.

11 | Euthanize mice by cervical dislocation and fixate enucleated eyes in 4% (w/v) PFA for no longer than 4 h at room temperature (RT  $\pm$  22°C).

▲ **CRITICAL STEP** This step must be performed by licensed and qualified individuals according to the animal welfare guidelines in the state.

## ? TROUBLESHOOTING

12 | Embed the eyes in optimal cutting temperature (OCT) compound for histological analysis of cryo sections (option A) or prepare eyes for flat mount analysis (option B)

### (A) Cryo sections • **TIMING 2 d**

(i) To dehydrate the tissue, place the fixated eyes in 30% sucrose over night at room temperature.

(ii) Embed eyes in cryomold® containers with OCT compound and use the gas phase of dry ice to freeze the embedded eye.

▲ **CRITICAL STEP** label the orientation of the eyes. During the cutting procedure it is important to know how the lens is oriented. Make sure that the containers stand straight during freezing.

■ **PAUSE POINT** embedded eyes can be stored until further processing at -80°C.

(iii) Cut eyes in 12  $\mu$ m sections in a cryostat.

▲ **CRITICAL STEP** Before starting with cutting, be sure that the orientation of the eye is correct. The cutting direction is from the optic nerve towards the lens. This is necessary to avoid that the loose lens damages the retinal structure during sectioning.

■ **PAUSE POINT** sections can be stored until further processing at -80°C.

(iv) Encircle the respective retinal cross sections with liquid barrier (Pink PAP Pen, Zytomed Systems) and let it dry.

▲ **CRITICAL STEP** Wait until the liquid barrier is completely dried, otherwise it may not be firmly attached to the slide and could detach which would interfere with staining.



(v) Rehydrate the cryo sections with 1x PBS for 15 min. Carefully remove the liquid using an exhaust pump.

(vi) | Incubate the cryo sections with Blotto for 30 min to prevent nonspecific binding.

## ? TROUBLESHOOTING

(vii) Carefully remove the liquid using an exhaust pump.

(viii) Incubate cryo sections with 50-100 µl primary antibody per section (Iba1, Wako, dilution 1:500). Incubate for 4h at RT or overnight at 4°C

(ix) Proceed the staining procedure by carefully remove liquid using an exhaust pump.

(x) Wash cryo sections three times with 1–2 ml 1x PBS, after 5 min of incubation carefully remove the PBS using an exhaust pump.

(xi) Incubate cryo sections with secondary antibody diluted in 1x PBS (goat anti-rabbit Alexa Flour 488, Thermo Scientific) for 1 h in the dark.

(xii) Wash cryo sections three times with 1–2 ml 1x PBS, after 5 min of incubation carefully remove the PBS using an exhaust pump

(xiii) Stain the nuclei with DAPI-solution (0.1 µg/ml in 1x PBS) for 10 min.

(xiv) Wash cryo sections three times by adding 1–2 ml 1x PBS, after 5 min of incubation carefully remove the PBS using an exhaust pump

(xv) Embed the fluorescently-labeled cryo sections in Dako and cover them with coverslips.

▲ **CRITICAL STEP** Avoid forming air bubbles.

■ **PAUSE POINT** Store the cryo sections in the dark at 2-8°C. It is recommended to analyze the fluorescently-labeled sections as soon as possible to avoid loss of fluorescence intensity.

(xvi) Analyze microglia location and morphology using an Axioskop 2 Fluorescence microscope or a confocal microscope.

The number of mononuclear phagocytes can be quantified by counting cells per section. Depending on the mouse model, mononuclear phagocytes can be located in different retinal layers such as the outer nuclear layer or the subretinal space (**Fig. 3**).

## **(B) Retinal flat mount analysis •TIMING 3 d**

**(i)** Transfer the fixed eye ball in a cell culture dish with 1x PBS and perform all dissection steps while the eye is submerged to avoid drying of the tissue.

**(ii)** Use Dumont #5 forceps to hold the eye at the optic nerve and spring scissors to remove the anterior part of the eye with a circular cut at the level of the *ora serrata*.

**(iii)** Remove the lens, iris and optic nerve and carefully press with the forceps at the posterior part of the sclera to separate the retina from the retinal pigment epithelium and sclera. Keep both, the retinal and RPE/scleral flat mounts for staining, as subretinal MPs can stick to either side.

**(iv)** Use spring scissors to cut the retina or the RPE/sclera in a four-leaf structure to avoid curling. Due to the natural shape of the retina, the tissue tends to curl up with the anterior retina inside (ganglion cell layer, inner plexiform and nuclear layer) and the posterior part (photoreceptor layer) outside. After flattening the tissue, the outer and inner retina can be distinguished by small pigmented particles of the RPE remaining at the retina.

▲ **CRITICAL STEP** To avoid tissue damage do not transfer the retina with forceps. Use a cropped transfer pipet and transfer tissue in a drop of 1x PBS.

## **? TROUBLESHOOTING**

**(v)** Incubate the flat mounts in the permeabilization solution on a see-saw rocker over night at 4°C.

▲ **CRITICAL STEP** Keep each retina and RPE/sclera in single wells to avoid agglutination of the tissue.

**(vi)** Incubate the flat mounts in BLOTTO on a see-saw rocker over night at 4°C or 4 h at room temperature to block nonspecific antigen-binding sites.

**(vii)** Incubate flat mounts with the primary antibody (Iba1, Wako, dilution 1:500) over night at 4°C.

**(viii)** Wash the tissue 3 times for at least 10 min in 1 ml 1x PBS on a see-saw rocker.

▲ **CRITICAL STEP** To achieve sufficient washing make sure that the tissue floats freely in 1x PBS.

**(ix)** Incubate the flat mounts with the secondary antibody diluted in 1x PBS (goat anti-rabbit Alexa Fluor 488, Thermo Scientific) for at least 1 h in the dark.

**(x)** Wash the tissue 3 times for at least 10 min in 1 ml 1x PBS on a see-saw rocker.

▲ **CRITICAL STEP** To achieve sufficient washing make sure that the tissue floats freely in 1x PBS.

**(xi)** Use a cropped transfer pipet to place the flat mount on a microscope slide (Superfrost® PLUS microscope slide, Fisher Scientific) with the vitreous side facing up and photoreceptor layer facing down.

(xii) Remove the remaining 1x PBS carefully with a tissue.

(xiii) Embed flat mounts with Fluorescent Mounting Medium (Dako) and cover glasses no.1 (18x18 mm, Th.Geyer).

▲ **CRITICAL STEP** To image neuroretinal phagocytes, mount the retinal tissue with the vitreous side facing up and the photoreceptor layer down. To image subretinal phagocytes at the photoreceptor outer segment layer, mount the retina with photoreceptor layer facing up and vitreous side down. To flat mount the RPE/sclera, extraocular tissues, such as conjunctiva, muscles, and optic nerve need to be completely removed.

■ **PAUSE POINT** Store embedded object slides at 4°C until further processing.

(xiv) To quantify microglial morphology examine the flat mount with a confocal microscope or a microscope equipped with an ApoTome device to depict the depth of the retinal tissue via optical sectioning (**Fig. 4**).

#### ? **TROUBLESHOOTING**

(xv) Use ImageJ to define a region of 200-500 µm diameter around the laser spot and use the same region to quantify all images belonging to one experiment (**Fig. 4c**).

(xvi) Count the number of round-shaped versus ramified mononuclear phagocytes (**Fig. 4d**).

▲ **CRITICAL STEP** This is a relatively subjective method to quantify microglial activation. Furthermore, there may be stained fragments that cannot be clearly defined as single cells with distinct amoeboid or ramified morphology. It is therefore highly recommended to additionally perform the grid cross method to verify the findings from counting amoeboid versus ramified microglia. For some pathologies including models for diabetic retinopathy, it may be also important to differentiate between parenchymal and perivascular mononuclear phagocytes.

(xvii) Use a grid system to determine the number of grid crossing points per cell<sup>34</sup>.

Open the grid plugin of ImageJ to overlay the image with a grid (**Fig. 4e, f**).

Count the number of grid crossing points per cell and calculate the mean grid crossed points per cell (**Fig. 4g**).

▲ **CRITICAL STEP** The grid in the image depends on the image size and pixel dimensions. To ensure the data is comparable between groups, the image size and resolution from all samples should be consistent.

## **Flow cytometry** • **TIMING 7 h**

**13** | Prepare solutions for flow cytometry. To dissociate retinal tissue prepare enzyme mix 1 and enzyme mix 2 according to the guidelines of the Neural Tissue Dissociation Kit - Postnatal neurons (Table 1).

**Table 1:** Enzyme mixes for tissue dissociation.

	Enzyme mix 1		Enzyme mix 2	
<b>Solution</b>	Enzyme P	Buffer Z	Buffer Y	Enzyme A
<b>multiple retinas (&lt;400mg)</b>	10 µl	1950 µl	30 µl	15 µl
<b>1-2 retinas</b>	5 µl	975 µl	15 µl	7.5 µl

**▲ CRITICAL STEP** For optimal results use a maximum of 400 mg of retinal tissue processed in 2 ml Enzyme mix for dissociation.

**▲ CRITICAL STEP** Add β-mercaptoethanol to Buffer Z at a final concentration of 0.067 mM. This solution will then be stable for 1 month at 4°C.

**▲ CRITICAL STEP** Re-suspend the lyophilized powder in the vial labeled Enzyme A with 1 ml of Buffer A. Do **not** vortex. This solution should then be aliquoted and stored at –20 °C for later use. Pre-warm Buffer Z to room temperature before use.

**14** | Euthanize mice by cervical dislocation and collect retinas in 1x PBS buffer on ice.

**▲ CRITICAL STEP** This step must be performed by licensed and qualified individuals according to the animal welfare guidelines in the state.

**▲ CRITICAL STEP** If using retinal tissues, all steps must be performed at room temperature

**15** | Crop a plastic transfer pipette, so that the opening has a diameter of approximately 0.4 mm

**▲ CRITICAL STEP** All tubes, cell strainers, and pipette tips should be rinsed with 1x PBS to avoid stickiness.

**16** | Transfer tissue into a 1.5 ml tube using a cropped plastic transfer pipette (0.4 mm)

**17** | Let tissue settle. Remove supernatant carefully.

**18** | Add 980 µl of **enzyme mix 1** (Table 1) to the retinas. Agitate gently to ensure that tissue is detached from the bottom of the tube.

**19** | Incubate in a closed 1.5 ml tube for 15 min at 37 °C under slow, continuous shaking using a Thermomixer compact (Eppendorf). Invert the tubes every 5 min manually.

**20** | Add 15 µl of **enzyme mix 2 (Table 1)**. Dissociate tissue using a wet cropped plastic transfer pipette (0.4 mm) by pipetting the whole solution up and down 10 x very carefully.

▲ **CRITICAL STEP** Use separate plastic transfer pipettes for each sample to avoid cross-contamination. Avoid forming air bubbles.

**21** | Incubate for 10 min at 37 °C under slow, continuous shaking using a Thermomixer compact (Eppendorf).

**22** | Add 7.5 µL of **enzyme mix 2 (Table 1)**. Dissociate tissue pieces using a wet cropped plastic transfer pipette (0.4 mm) by pipetting up and down 10 x very carefully. Dissociate tissue pieces further using a plastic transfer pipette, with its **original** opening, by pipetting approximately 1 ml up and down 40 x very carefully and slowly.

▲ **CRITICAL STEP** Use separate plastic transfer pipettes for each sample to avoid cross-contamination. Avoid forming air bubbles. Do not vortex.

#### ? TROUBLESHOOTING

**23** | Apply the cell suspension to a tube with 70 µm cell strainer. Carefully add 4 ml of 1x PBS and rinse all cells through the strainer.

**24** | Centrifuge at 130 x g for 10 min. Remove supernatant carefully

**25** | Resuspend cells carefully in 1x PBS to required volume by pipetting slowly up and down using a 1 ml pipette tip. Do not vortex the cells.

**26** | Count cells (dilution 1:100) using a Neubauer chamber. Prepare cell suspension with desired concentration of nucleated cells.

**27** | Use Viability 405/452 <sup>TM</sup> Fixable Dye (Miltenyi biotec) to exclude dead cells from analysis.

▲ **CRITICAL STEP** For compensation: If a low number of dead cells is expected, then it is recommended to heat-kill cells (95°C for 5 min). Be aware that fixable viability dye also binds to a low amount to live cells (live cells can also have a shift in fluorescent intensity compared to unstained cells) if you analyze flow cytometry data.

**28** | Prepare cells in tubes. Wash cells 2 x with azide-free and serum/protein-free 1x PBS. Centrifuge cell suspension at 300xg for 10 min. Discard supernatant completely. ▲ **CRITICAL STEP** Make sure that you use 1x PBS free of azide, protein and any other amine-containing solution, because Viability Fixable Dyes react with primary amine groups of proteins.

**29** | Resuspend up to 1x10<sup>7</sup> cells in 100µl azide-free and serum/protein-free 1x PBS. Add 1 µl of Viability 405/452 <sup>TM</sup> Fixable Dye.

**30** | Mix well and incubate for 15 minutes in the dark at room temperature. **▲ CRITICAL STEP** Note that higher temperatures or longer incubation time may lead to nonspecific binding. Working at low temperatures or on ice requires prolonged incubation time.

**31** | Wash cells 1-2 x with FACS buffer and proceed with further staining.

**32** | Centrifuge cell suspension at 300xg for 10 min at 4°C. Discard supernatant and proceed with Fc receptor (FcR) blocking and staining of surface antigens.

**33** | To increase specificity of antibody labeling block nonspecific binding to FC receptor (FcR). To block FcR resuspend up to  $1 \times 10^7$  cells in 90  $\mu$ l FACS buffer and add 10 $\mu$ l of FcR Blocking Reagent.

**34** | Incubate for 10 minutes at 2-8°C.

**35** | Proceed with staining of the surface antigen CD11b<sup>+</sup>. Add 10 $\mu$ l CD11b<sup>+</sup> - APC antibody (up to  $1 \times 10^7$  cells in 100  $\mu$ l FACS buffer containing FcR Blocking reagent , dilution:1:11) to the cell suspension . To examine nonspecific binding of the CD11b<sup>+</sup> antibody, include an isotype control staining. Instead of using CD11b<sup>+</sup> antibody, add 10  $\mu$ l Rat IgG2b isotype control antibody conjugated to APC (up to  $2 \times 10^6$  cells in 100  $\mu$ l FACS buffer containing FcR Blocking reagent ).

**▲ CRITICAL STEP** Cells should be stained prior to fixation if formaldehyde is used as a fixative.

**▲ CRITICAL STEP** Buffers containing Ca<sup>2+</sup> or Mg<sup>2+</sup> are not recommended for surface antigen staining and flow cytometry.

**▲ CRITICAL STEP** Note that higher temperatures or longer incubation time may lead to nonspecific binding.

**36** | Mix well and incubate for further 10 min in the dark at 2–8°C.

**▲ CRITICAL STEP** Higher temperature or longer incubation may lead to nonspecific labelling.

**37** | Wash cells with FACS buffer (1-2 ml). Centrifuge cell suspension at 300xg for 10 min. Discard supernatant.

**38** | Resuspend cell pellet in a suitable amount of FACS buffer (100-200 $\mu$ l) for analysis or proceed with fixation (optional). Fixation of the cells is recommended, if the analysis cannot be performed immediately after the staining procedure.

**39** | Centrifuge cell suspension at 300xg for 10 min. Discard supernatant. For cell fixation, use 0.5 ml fixation buffer per tube (Fluoro Fix Buffer). Incubate cells in the dark for 30 min. **! CAUTION** The fixation buffer contains paraformaldehyde, which is toxic and mutagenic.

**40** | Wash cells by adding 1–2 ml of FACS buffer and centrifuge at 300×g for 10 min. Aspirate supernatant completely.

**41** | Resuspend cell pellet in a suitable amount of FACS buffer (100-200µl) for flow cytometry analysis.

■ **PAUSE POINT** Store tube until analysis at 2-8°C in the dark covered with parafilm. Proceed with the analysis as soon as possible.

**42** | Quantify the number of CD11b<sup>+</sup> cells by flow cytometry (e.g. using a FACS Canto II).

**43** | Gating strategy: Exclude doublets and dead cells. Perform frequency analysis of CD11b<sup>+</sup> cells using the Flowjo software (Fig. 5a, b, c) (Supplementary Fig. 1 a). Include Isotype controls to examine nonspecific binding. Use heat-killed cells as positive control for live/dead cell analysis (Supplementary Fig. 1 b, c). **Limitations:** The relative percentage and number of cells per retina can be accurately quantified. However, information about location and morphology are missing. This protocol it is not suitable to differentiate between resident retinal immune and invading myeloid cells from the circulation such as monocytes or neutrophils.

## Gene expression • **TIMING 8 h**

**44** | Prepare RNase-free lysis buffer (from the RNA extraction kit) on ice by adding β-Mercaptoethanol.

**45** | Euthanize mice, by cervical dislocation and collect retinas in 1x PBS buffer on ice

▲ **CRITICAL STEP** This step must be performed by licensed and qualified individuals according to the animal welfare guidelines in the state.

**46** | Pool both retinas of one animal and transfer to a 2.0 ml reaction tube with RNase-free lysis buffer and add stainless steel beads (5 mm diameter, Qiagen).

**47** | Homogenize retinal tissue for 1 min at 50/s using a TissueLyser LT homogenizer (Qiagen).

**48** | Centrifuge homogenized tissue for 5 min at full speed, discard pellet and proceed with the supernatant.

▲ **CRITICAL STEP** If samples became hot during mechanical homogenization, precool buffers and steel beads and store samples on ice.

49 | Isolate total RNA with the NucleoSpin® RNA Mini Kit (Macherey-Nagel) according to the manufacturer's protocol.

50 | Dissolve RNA with 30 µl of RNase-free water.

51 | Measure RNA concentration with a NanoDrop 2000 Spectrophotometer (Thermo Scientific).

▲ **CRITICAL STEP** Always work under RNase-free conditions.

▲ **CRITICAL STEP** Pool several retinas if poor RNA yield is obtained.

## ? TROUBLESHOOTING

■ **PAUSE POINT** Store RNA at -80°C until further use.

52 | Reverse transcribe RNA into cDNA with the RevertAid™ RT Kit (Thermo Scientific) or comparable kit according to the manufacturer's manual.

■ **PAUSE POINT** Store cDNA at -20°C until further use.

53 | Dilute cDNA with RNase-free water to a final concentration of 20 ng/µl.

54 | Prepare 7.5 µl reaction mix per sample containing 5 µl 1x TaqMan Gene Expression Master Mix (Invitrogen Life Technologies), 1 µl forward primer (200 nM), 1 µl reverse primer (200 nM), 0.125 µl dual-labeled probe (Roche Universal Probe Library, Roche) and 0.375 µl distilled water (**Table 2**).

**Table 2:** Primers and Roche probes for quantitative real-time PCR.

Gene	Direction	Sequence	Probe
<b>Atp5b</b>	forward	5'-GGCACAATGCAGGAAAGG-3'	#77
	reverse	5'-TCAGCAGGCACATAGATAGCC-3'	
<b>Amwap</b>	forward	5'-TTTGATCACTGTGGGGATGA-3'	#1
	reverse	5'-ACACTTTCTGGTGAAGGCTTG-3'	
<b>Ccl2</b>	forward	5'-CATCCACGTGTTGGCTCA-3'	#62
	reverse	5'-GATCATCTTGCTGGTGAATGAGT-3'	

55 | Pipette 2.5 µl cDNA into each well of a FrameStar® 384 PCR plate and add 7.5 µl reaction mix so that the final cDNA concentration is 50 ng per reaction well.

56 | Centrifuge plate for 5 min with 900 rpm.

■ **PAUSE POINT** Store PCR plates at 4°C in the dark until run is performed.



**57** | Run the real time PCR reaction with following reaction parameters: 10 min at 95°C followed by 40 cycles of 15 sec at 95°C melting and 1 min 60°C annealing/extension.

**58** | Analyze the results by using the  $\Delta\Delta C_t$  method for relative quantification (**Fig. 6a-c**)<sup>54</sup>.

**▲ CRITICAL STEP** Prepare 10 % more reaction mix to compensate for pipetting loss.

## ●TIMING

Steps 1-5, Funduscopy: 15 min per mouse

Steps 6-12, Immunohistochemistry - Reagent setup: 4.5 h

Steps 12 A Cryo sections: 2 d

Steps 12 B Flat mounts: 3 d

Steps 13-43, Flow cytometry: 7 h

Steps 44-58, Gene expression: 8 h

## ? TROUBLESHOOTING

**Table 3:** Troubleshooting.

Step	Problem	Possible reason	Solution
1	Dull lens	Mice are under anesthetic for too long.	Anesthetize animal shortly before <i>in vivo</i> analysis.
	Death of mice	Overdose of anesthetic.	Weigh animal before injection to calculate optimal dose.
2	Insufficient insight in fundus	Pupil is not entirely dilated.	Wait a few minutes until the Iris dilator muscle is completely relaxed. Make sure that the Phenylephrin/ Tropicamid mixture has not past passed its expiration date.
3	Poor <i>in vivo</i> image quality	Light cannot enter the eye and/or reflection is not collected properly.	Change the position of the animal in front of the objective.
4,5	Blurry fundus insight	Sclera is too dry.	Use artificial tear drops or 0.9% (w/v) NaCl to moisten sclera.
11	Nonspecific staining	Antigen conformation has changed	Reduce time of fixation to preserve natural protein structures.
12 A (vi)	High background staining	Insufficient washing or old BLOTTO solution.	Extend washing time when background staining is too prominent. Prepare fresh BLOTTO solution each time right before use.
12 B (iv)	Irregular stained retina	Tissue is curled up during staining procedure	Cut the retina in a four-leaf structure before starting the staining protocol.

<b>12 B (xiv)</b>	Insufficient image quality	Objective quality, microscope equipment	To define microglia distribution in the different retinal layers, imaging the flat mount in z-stacks is highly recommended. When using the Axioskop2 MOT Plus Apotome microscope (Carl Zeiss) it is recommended to use the Plan-Apochromat objective 20x/0.8 M27 (No. 420650-9901-000, Carl Zeiss)
<b>22</b>	Retina is poorly dissociated	The diameter of the cropped transfer pipette is too big.	Crop the transfer pipette at different areas to vary the diameter. Try to use different diameters and continue pipetting the tissue up and down. It may take some time until the tissue is completely dissociated; continue until you have a single cell suspension.
<b>51</b>	Low RNA quality	Tissue sample has been stored too long.	Process tissue as fast as possible and, if necessary, store tissue at -80°C.
<b>51</b>	Low RNA quantity	RNA has been degraded	Make sure you use RNase-free reagents and material.

## ANTICIPATED RESULTS

Reactivity of mononuclear phagocytes is a general hallmark of the innate immune response occurring in various degenerative and inflammatory retinal disorders. In this protocol, we outline comprehensive methods to characterize the most important aspects of mononuclear phagocyte biology in the mouse retina. Fluorescently labelled microglia can be visualized *in vivo* with confocal scanning laser ophthalmoscopy (**Fig. 2**). The location and distribution of mononuclear phagocytes can be defined by counting Iba1- cells in retinal cryo sections as shown for a genetic model of retinal degeneration (**Fig. 3 a-d**) and for a white light damage paradigm (**Fig. 3 e-h**). The overall cell morphology in the regularly spaced network is then characterized in retinal flat mounts stained with Iba1 (**Fig. 4 a,b**). The activation status of mononuclear cells in a laser lesion is described by counting the number of ramified (asterisks) versus amoeboid cells (circles) in a defined area (**Fig. 4 c,d**) and the cell morphology can be further verified by grid cross analysis (**Fig. 4 e-g**). The relative percentage of retinal mononuclear phagocytes can be determined by flow cytometry gating on CD11b<sup>+</sup> live cells (**Fig. 5 a-d**). The expected relative percentage of live cells and CD11b<sup>+</sup> cells in the healthy retina should be more than 70% and less than 1%, respectively (**Fig. 5 a,b**). In the light damage model, the number of live cells stays approximately the same, whereas the population of mononuclear phagocytes increases up to 3.4% (**Fig. 5 a-d**). The percentage of mononuclear phagocytes varies between disease models and time points. The gating strategy shows how to precisely analyze the amount of CD11b<sup>+</sup> cells after excluding doublets and dead cells (**Supplementary Fig. 1 a**). Additionally, the staining controls for flow cytometry demonstrate a specific signal of CD11b-APC antibody compared to isotype and FMO controls (**Supplementary Fig. 1 b,c**). The magnitude of mononuclear phagocyte activation can be measured with quantitative RT-PCR analysis of the markers AMWAP and CCL2, applied here to retinas with Fam161a mutation<sup>39</sup>, in the laser-CNV model<sup>44</sup>, and in a white light damage model<sup>32, 33</sup> (**Fig. 6 a-c**).

## Acknowledgments

This work was supported by grants from the DFG (LA1203/6-2, LA1203/9-1, LA1203/10-1, and FOR2240), the ProRetina Foundation, the Hans and Marlies Stock Foundation, the Velux Foundation, Fight for Sight (1425/1426), the BMBF (03VP00272), the Graduate Program in Pharmacology and Experimental Therapeutics at the University of Cologne in collaboration with Bayer AG, grants from INSERM, ANR MACLEAR (ANR-15-CE14-0015-01), LABEX LIFESENSES [ANR-10-LABX-65], the ANR (Investissements d'Avenir programme [ANR-11-IDEX-0004-02]), Carnot, ERC starting Grant (ERC-2007 St.G. 210345) and by Association de Prévoyance Santé de ALLIANZ.

### **Author contributions**

AL and RS performed experiments, analyzed the data and wrote the manuscript. FS and HX designed the research and corrected the manuscript. TL designed the research, obtained the funding, and finalized the manuscript. All authors read and approved the final manuscript. All authors have worked on and optimized this protocol.

### **Competing financial interests**

The authors declare no competing financial interest.

## REFERENCES

1. Reichenbach, A. & Bringmann, A. New functions of Muller cells. *Glia* **61**, 651-678 (2013).
2. Vecino, E., Rodriguez, F.D., Ruzafa, N., Pereiro, X. & Sharma, S.C. Glia-neuron interactions in the mammalian retina. *Progress in retinal and eye research* **51**, 1-40 (2016).
3. Thanos, S., Moore, S. & Hong, Y. Retinal Microglia. *Progress in retinal and eye research* **15**, 331-361 (1996).
4. Hume, D.A., Perry, V.H. & Gordon, S. Immunohistochemical localization of a macrophage-specific antigen in developing mouse retina: phagocytosis of dying neurons and differentiation of microglial cells to form a regular array in the plexiform layers. *J Cell Biol* **97**, 253-257 (1983).
5. Liang, K.J., *et al.* Regulation of dynamic behavior of retinal microglia by CX3CR1 signaling. *Investigative ophthalmology & visual science* **50**, 4444-4451 (2009).
6. Lee, J.E., Liang, K.J., Fariss, R.N. & Wong, W.T. Ex vivo dynamic imaging of retinal microglia using time-lapse confocal microscopy. *Investigative ophthalmology & visual science* **49**, 4169 (2008).
7. Karlstetter, M., *et al.* Retinal microglia: just bystander or target for therapy? *Progress in retinal and eye research* **45**, 30-57 (2015).
8. Madeira, M.H., Boia, R., Santos, P.F., Ambrosio, A.F. & Santiago, A.R. Contribution of microglia-mediated neuroinflammation to retinal degenerative diseases. *Mediators Inflamm* **2015**, 673090 (2015).
9. Zabel, M.K., *et al.* Microglial phagocytosis and activation underlying photoreceptor degeneration is regulated by CX3CL1-CX3CR1 signaling in a mouse model of retinitis pigmentosa. *Glia* **64**, 1479-1491 (2016).
10. Zhao, L., *et al.* Microglial phagocytosis of living photoreceptors contributes to inherited retinal degeneration. *EMBO molecular medicine* **7**, 1179-1197 (2015).
11. Dannhausen, K., *et al.* Acid sphingomyelinase (aSMase) deficiency leads to abnormal microglia behavior and disturbed retinal function. *Biochemical and biophysical research communications* **464**, 434-440 (2015).
12. Combadiere, C., *et al.* CX3CR1-dependent subretinal microglia cell accumulation is associated with cardinal features of age-related macular degeneration. *J.Clin.Invest* **117**, 2920-2928 (2007).
13. Xu, H., Chen, M., Mayer, E.J., Forrester, J.V. & Dick, A.D. Turnover of resident retinal microglia in the normal adult mouse. *Glia* **55**, 1189-1198 (2007).
14. Sennlaub, F., *et al.* CCR2(+) monocytes infiltrate atrophic lesions in age-related macular disease and mediate photoreceptor degeneration in experimental subretinal inflammation in Cx3cr1 deficient mice. *EMBO molecular medicine* **5**, 1775-1793 (2013).
15. Luckoff, A., *et al.* Interferon-beta signaling in retinal mononuclear phagocytes attenuates pathological neovascularization. *EMBO Mol Med* **8**, 670-678 (2016).
16. O'Koren, E.G., Mathew, R. & Saban, D.R. Fate mapping reveals that microglia and recruited monocyte-derived macrophages are definitively distinguishable by phenotype in the retina. *Scientific reports* **6**, 20636 (2016).
17. Bodeutsch, N. & Thanos, S. Migration of phagocytotic cells and development of the murine intraretinal microglial network: an in vivo study using fluorescent dyes. *Glia* **32**, 91-101 (2000).
18. Eter, N., *et al.* In vivo visualization of dendritic cells, macrophages, and microglial cells responding to laser-induced damage in the fundus of the eye. *Invest Ophthalmol Vis Sci* **49**, 3649-3658 (2008).
19. Sasmono, R.T., *et al.* A macrophage colony-stimulating factor receptor-green fluorescent protein transgene is expressed throughout the mononuclear phagocyte system of the mouse. *Blood* **101**, 1155-1163 (2003).

20. Joly, S., *et al.* Cooperative phagocytes: resident microglia and bone marrow immigrants remove dead photoreceptors in retinal lesions. *The American journal of pathology* **174**, 2310-2323 (2009).
21. Crespo-Garcia, S., *et al.* In vivo analysis of the time and spatial activation pattern of microglia in the retina following laser-induced choroidal neovascularization. *Experimental eye research* **139**, 13-21 (2015).
22. Karlstetter, M., Ebert, S. & Langmann, T. Microglia in the healthy and degenerating retina: insights from novel mouse models. *Immunobiology* **215**, 685-691 (2010).
23. Luhmann, U.F., *et al.* Ccl2, Cx3cr1 and Ccl2/Cx3cr1 chemokine deficiencies are not sufficient to cause age-related retinal degeneration. *Experimental eye research* **107**, 80-87 (2013).
24. Xu, H., Chen, M., Manivannan, A., Lois, N. & Forrester, J.V. Age-dependent accumulation of lipofuscin in perivascular and subretinal microglia in experimental mice. *Aging cell* **7**, 58-68 (2008).
25. Ebert, S., *et al.* Docosahexaenoic acid attenuates microglial activation and delays early retinal degeneration. *Journal of neurochemistry* **110**, 1863-1875 (2009).
26. Gramlich, O.W., *et al.* Immune response after intermittent minimally invasive intraocular pressure elevations in an experimental animal model of glaucoma. *Journal of neuroinflammation* **13**, 82 (2016).
27. Kambhampati, S.P., *et al.* Systemic and Intravitreal Delivery of Dendrimers to Activated Microglia/Macrophage in Ischemia/Reperfusion Mouse Retina. *Investigative ophthalmology & visual science* **56**, 4413-4424 (2015).
28. Miloudi, K., *et al.* Truncated netrin-1 contributes to pathological vascular permeability in diabetic retinopathy. *The Journal of clinical investigation* **126**, 3006-3022 (2016).
29. Kezic, J.M., Chen, X., Rakoczy, E.P. & McMenamin, P.G. The effects of age and Cx3cr1 deficiency on retinal microglia in the Ins2(Akita) diabetic mouse. *Investigative ophthalmology & visual science* **54**, 854-863 (2013).
30. Koso, H., *et al.* Conditional rod photoreceptor ablation reveals Sall1 as a microglial marker and regulator of microglial morphology in the retina. *Glia* (2016).
31. Zhao, L., Ma, W., Fariss, R.N. & Wong, W.T. Minocycline attenuates photoreceptor degeneration in a mouse model of subretinal hemorrhage microglial: inhibition as a potential therapeutic strategy. *The American journal of pathology* **179**, 1265-1277 (2011).
32. Scholz, R., *et al.* Targeting translocator protein (18 kDa) (TSPO) dampens pro-inflammatory microglia reactivity in the retina and protects from degeneration. *Journal of neuroinflammation* **12**, 201 (2015).
33. Scholz, R., *et al.* Minocycline counter-regulates pro-inflammatory microglia responses in the retina and protects from degeneration. *Journal of neuroinflammation* **12**, 209 (2015).
34. Chen, M., *et al.* Para-inflammation-mediated retinal recruitment of bone marrow-derived myeloid cells following whole-body irradiation is CCL2 dependent. *Glia* **60**, 833-842 (2012).
35. Zhao, J., Chen, M. & Xu, H. Experimental autoimmune uveoretinitis (EAU)-related tissue damage and angiogenesis is reduced in CCL2(-)/(-)CX(3)CR1gfp/gfp mice. *Investigative ophthalmology & visual science* **55**, 7572-7582 (2014).
36. Wu, W.K., *et al.* IL-4 regulates specific Arg-1(+) macrophage sFlt-1-mediated inhibition of angiogenesis. *The American journal of pathology* **185**, 2324-2335 (2015).
37. Karlstetter, M., *et al.* The novel activated microglia/macrophage WAP domain protein, AMWAP, acts as a counter-regulator of proinflammatory response. *J Immunol* **185**, 3379-3390 (2010).
38. Aslanidis, A., *et al.* Activated microglia/macrophage whey acidic protein (AMWAP) inhibits NFkappaB signaling and induces a neuroprotective phenotype in microglia. *Journal of neuroinflammation* **12**, 77 (2015).
39. Karlstetter, M., *et al.* Disruption of the retinitis pigmentosa 28 gene Fam161a in mice affects photoreceptor ciliary structure and leads to progressive retinal degeneration. *Human molecular genetics* **23**, 5197-5210 (2014).

40. Levy, O., *et al.* APOE Isoforms Control Pathogenic Subretinal Inflammation in Age-Related Macular Degeneration. *J Neurosci* **35**, 13568-13576 (2015).
41. Muller, U., *et al.* Functional role of type I and type II interferons in antiviral defense. *Science* **264**, 1918-1921 (1994).
42. Caspi, R.R. Understanding autoimmunity in the eye: from animal models to novel therapies. *Discovery medicine* **17**, 155-162 (2014).
43. Zeiss, C.J. Animals as models of age-related macular degeneration: an imperfect measure of the truth. *Vet Pathol* **47**, 396-413 (2010).
44. Lambert, V., *et al.* Laser-induced choroidal neovascularization model to study age-related macular degeneration in mice. *Nat Protoc* **8**, 2197-2211 (2013).
45. Connor, K.M., *et al.* Quantification of oxygen-induced retinopathy in the mouse: a model of vessel loss, vessel regrowth and pathological angiogenesis. *Nature protocols* **4**, 1565-1573 (2009).
46. Chang, B., *et al.* Mouse models of ocular diseases. *Visual neuroscience* **22**, 587-593 (2005).
47. Fernandes, K.A., *et al.* Using genetic mouse models to gain insight into glaucoma: Past results and future possibilities. *Experimental eye research* **141**, 42-56 (2015).
48. Grimm, C. & Reme, C.E. Light damage as a model of retinal degeneration. *Methods in molecular biology (Clifton, N.J.)* **935**, 87-97 (2013).
49. Carter, D.A., Balasubramaniam, B. & Dick, A.D. Functional analysis of retinal microglia and their effects on progenitors. *Methods in molecular biology (Clifton, N.J.)* **935**, 271-283 (2013).
50. Langmann, T. Microglia activation in retinal degeneration. *J.Leukoc.Biol.* **81**, 1345-1351 (2007).
51. Poor, S.H., *et al.* Reliability of the mouse model of choroidal neovascularization induced by laser photocoagulation. *Invest Ophthalmol Vis Sci* **55**, 6525-6534 (2014).
52. D'Mello, C., Le, T. & Swain, M.G. Cerebral microglia recruit monocytes into the brain in response to tumor necrosis factor alpha signaling during peripheral organ inflammation. *J Neurosci* **29**, 2089-2102 (2009).
53. Ma, W., *et al.* Gene expression changes in aging retinal microglia: relationship to microglial support functions and regulation of activation. *Neurobiology of aging* **34**, 2310-2321 (2013).
54. Livak, K.J. & Schmittgen, T.D. Analysis of relative gene expression data using real-time quantitative PCR and the 2(-Delta Delta C(T)) Method. *Methods (San Diego, Calif.)* **25**, 402-408 (2001).
55. Kilkenny, C., Browne, W.J., Cuthill, I.C., Emerson, M. & Altman, D.G. Improving bioscience research reporting: the ARRIVE guidelines for reporting animal research. *Osteoarthritis and cartilage* **20**, 256-260 (2012).

## Figure legends

### **Figure 1. Diagram illustrating the comprehensive microglia characterization procedure.**

The protocol includes *in vivo* funduscopy as first step followed by *in situ* analyses including immunohistochemistry, flow cytometry, and gene expression.

### **Figure 2. Funduscopy of C57BL6/J mice (a, b) and MacGreen mice (c, d) mice**

after laser-treatment of the retina imaging infrared (IR) and blue autofluorescence (BAF) with an excitation wavelength of 488 nm. The lesion area is visible in both mouse lines in the IR channel (a,c), whereas EGFP-labeled microglia are only detectable in MacGreen reporter mice (d; BAF channel). White dashed circles highlight the area of the laser spot. For this method 8 to 10 weeks old female mice have been used and the experiment was approved by the governmental body responsible for animal welfare in the state of North Rhine-Westphalia, Germany with the permission number Az 84-02-04-2015-A039 and followed the ARRIVE guidelines<sup>55</sup>.

### **Figure 3. Immunohistochemical analyses of microglia in retinal cross sections. (a)**

Iba1-immunolabeled and DAPI counterstained cryo section of a healthy C57BL6/J control mouse retina shows ramified microglia cells located in the outer plexiform layer (OPL) and inner plexiform layer (IPL). (b) Image of a Fam161a<sup>GT/GT</sup> mouse retina at an early postnatal time point shows microglia starting to infiltrate into the degenerating outer nuclear layer (ONL). (c) In a later stage of degeneration, amoeboid reactive microglia accumulate in the OPL and subretinal space. (d) Quantification of retinal microglia distribution by counting the number of Iba1+ cells in the ONL and subretinal space per each section. (n = 1 exemplary image). (e) Ramified microglia cells in untreated Balb/c control mouse. (f) Amoeboid reactive microglia migrate into the ONL one day after light-exposure. (g) Iba1+ cells are found into the subretinal space four days post light-damage. (n = 1 exemplary image). (h) Quantification of retinal microglia distribution by counting the number of Iba1+ cells in the ONL and subretinal space per each section. For the experiments male and female mice with an age between 4 and 12 weeks have been used and the experiments were approved by the governmental body responsible for animal welfare in the state of North Rhine-Westphalia, Germany with the permission numbers Az 84-02.05.20.12.158 and Az 84-02-04-2015-A039 and followed the ARRIVE guidelines<sup>55</sup>.

### **Figure 4. Immunohistochemical analyses of microglia in retinal flat mounts. (a)**

C57BL6/J control mouse retina shows a network of ramified Iba1+ microglia in the plexiform layers. (b) The network is lost and amoeboid cells replace the ramified cells in degenerating

Fam161a<sup>GT/GT</sup> mouse retinas. (c) Amoeboid (circles) and ramified (asterisks) microglia accumulate in the lesion of the laser-CNV model. (d) Counting of ramified and amoeboid-shaped microglia cells in a laser lesion. (n = 1 exemplary image). (e-g) Grid cross analysis to determine ramified (e) and amoeboid (f) cell morphology by counting the number of grid crossing points per cell. Bars show mean  $\pm$  SD (n = 2-3 cells) (g). For the experiments male and female mice with an age between 8 and 12 weeks have been used and the experiments were approved by the governmental body responsible for animal welfare in the state of North Rhine-Westphalia, Germany with the permission numbers Az 84-02.05.20.12.158 and Az 84-02-04-2014-A466 and followed the ARRIVE guidelines<sup>55</sup>.

**Figure 5. Flow cytometry analysis of retinal microglia.** (a, b, top images) Flow cytometry to determine the percentage of living cells after retinal dissociation and staining. Only living, single cells are included in the further analysis of CD11b<sup>+</sup> cells. (a, b bottom images) CD11b<sup>+</sup> staining shows a low percentage of mononuclear phagocytes in the retina of a healthy control mouse. (a, bottom image) The percentage of CD11b<sup>+</sup> cells increases significantly in retinas four days after light exposure (b, bottom image). The graph shows the percentage of CD11b<sup>+</sup> cells per 500 000 analyzed cells. Mice exposed to bright white light show a significant higher percentage of CD11b<sup>+</sup> cells. Data show mean  $\pm$  SD \*\*p < 0.0074 (c) The graph shows the number of CD11b<sup>+</sup> cells per 500 000 analyzed cells. Mice exposed to bright white light show a significant higher number of CD11b<sup>+</sup> cells. Data show mean  $\pm$  SD \*\*p < 0.008 (d). Flow cytometry data were analyzed using an unpaired Student's t-test. (control n=5, light-damage n=5), one data point indicates the percentage or number of CD11b<sup>+</sup> cells from both retinas of one individual mouse, respectively. Male Balb/c mice with an age between 16 and 20 weeks were used for flow cytometry analysis. The use of mice in this experiment was approved by the governmental body responsible for animal welfare in the state of North Rhine-Westphalia, Germany with the permission number Az 84-02-04-2015-A039 and followed the ARRIVE guidelines<sup>55</sup>.

**Figure 6. RT-PCR analyses of representative microglia activation marker genes.** Activated microglia wavy acidic protein (AMWAP) and CC-chemokine ligand 2 (CCL2) are reliable marker genes that reflect microglia reactivity in the Fam161a<sup>GT/GT</sup> degeneration model (a), in experimental laser-coagulation (b) and in the light-damage model of retinal degeneration (c). Data show mean  $\pm$  SD (genetic model: n = 3-6, laser-CNV model: n = 3-4, light-damage model: n = 8-15, samples measured in duplicates). The data were analyzed used the Student's t-test (\*p > 0.01, \*\*p > 0.001, \*\*\*p > 0.0001). For the experiments male and female Balb/cJ,



C57BL6/J or Fam161<sup>GT/GT</sup> mice with an age between 8 and 12 weeks were used and the experiments were approved by the governmental body responsible for animal welfare in the state of North Rhine-Westphalia, Germany with the permission numbers Az 84-02.05.20.12.158, Az 84-02-04-2014-A466 and Az 84-02-04-2015-A039 and followed the ARRIVE guidelines<sup>55</sup>.

**Supplementary Figure 1. Gating Strategy and staining controls for flow cytometry analysis.** Representative FACS plots of a healthy control **(a)**. Doublets and dead cells were excluded from analysis by determination of a single and a live gate. Afterwards the amount of CD11b<sup>+</sup> cells can be analyzed **(a)**. To determine a live gate, it is necessary to include an unstained control and heat-killed, Viability<sup>TM</sup> fixable dye stained control **(b)**. To exclude nonspecific labeling of the CD11b<sup>+</sup> antibody and to determine the CD11b<sup>+</sup> gate, it is necessary to include Fluorescence minus one (FMO) controls without CD11b<sup>+</sup> (FMO sample is labeled with FcR blocking reagent and Viability<sup>TM</sup> fixable dye) and isotype controls **(c)**. (n=1 representative image). Male Balb/c mice with an age between 16 and 20 weeks were used for flow cytometry analysis. The use of mice in this experiment was approved by the governmental body responsible for animal welfare in the state of North Rhine-Westphalia, Germany with the permission numbers Az 84-02.05.20.12.158, Az 84-02-04-2014-A466 and Az 84-02-04-2015-A039 and followed the ARRIVE guidelines<sup>55</sup>.

Figure 1: Diagram illustrating the comprehensive microglia characterization procedure.

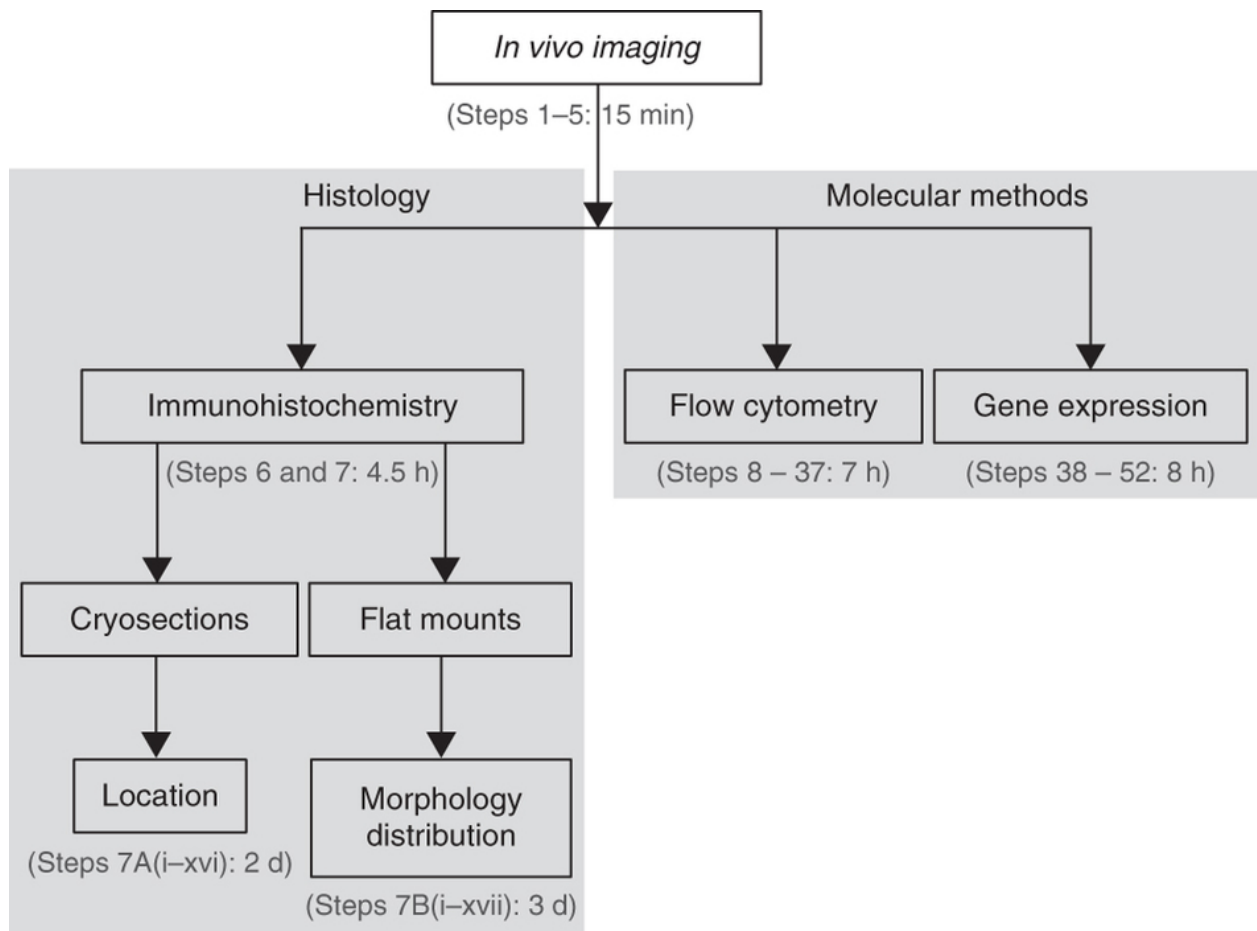


Figure 2: Retinal *in vivo* imaging of mice.

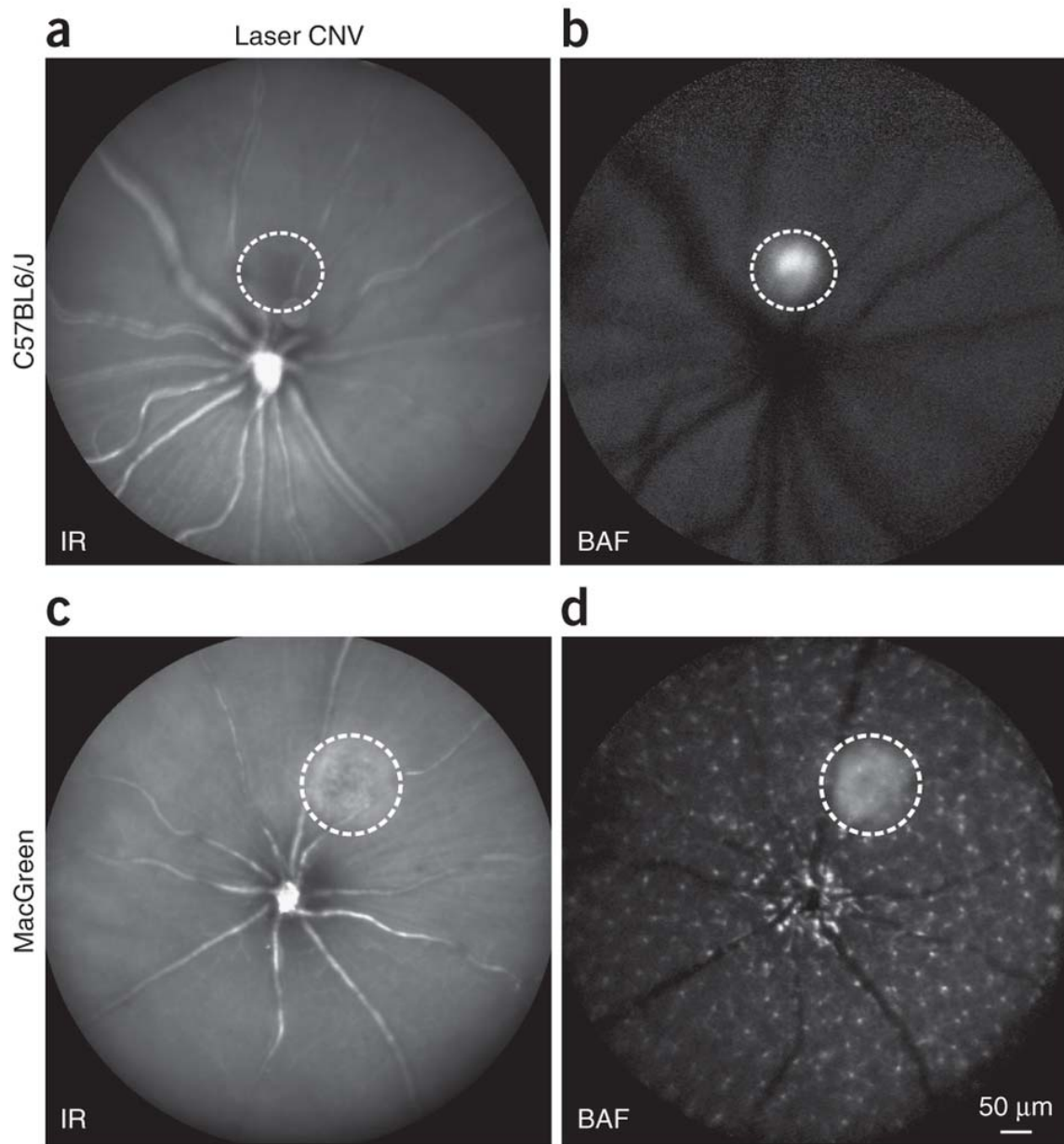


Figure 3: Immunohistochemical analyses of microglia in retinal cross-sections.

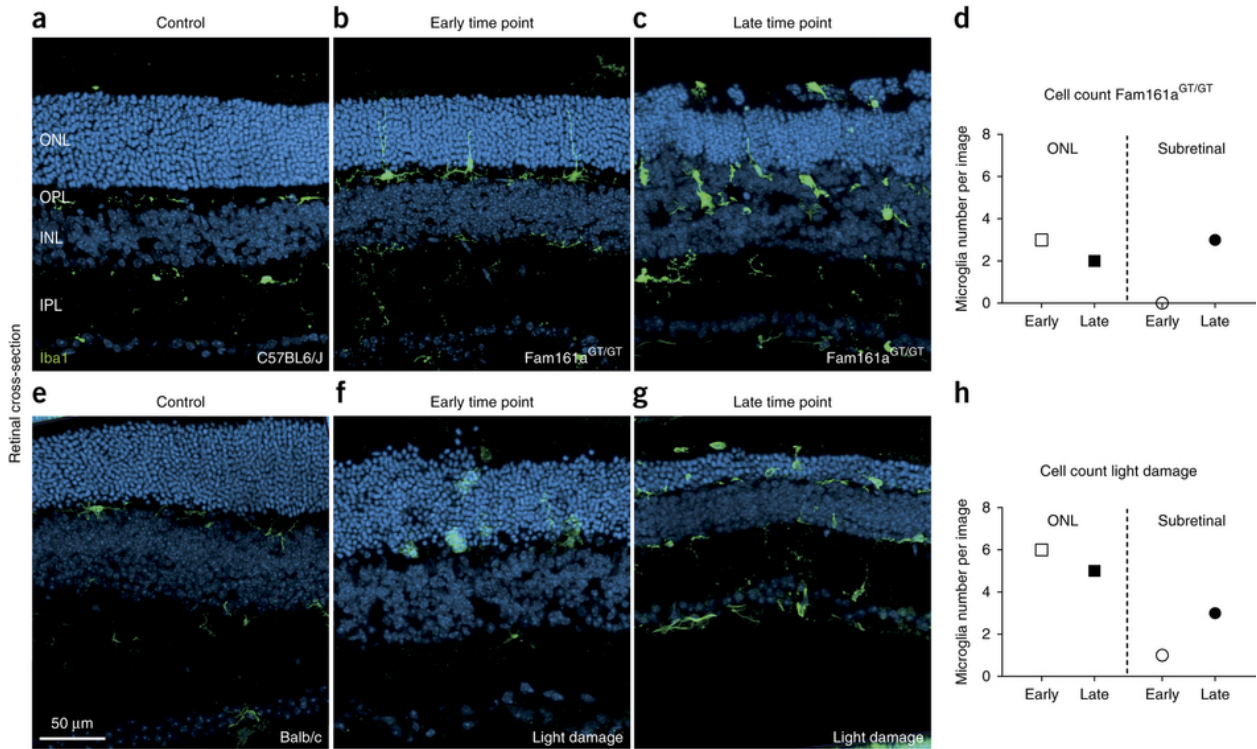
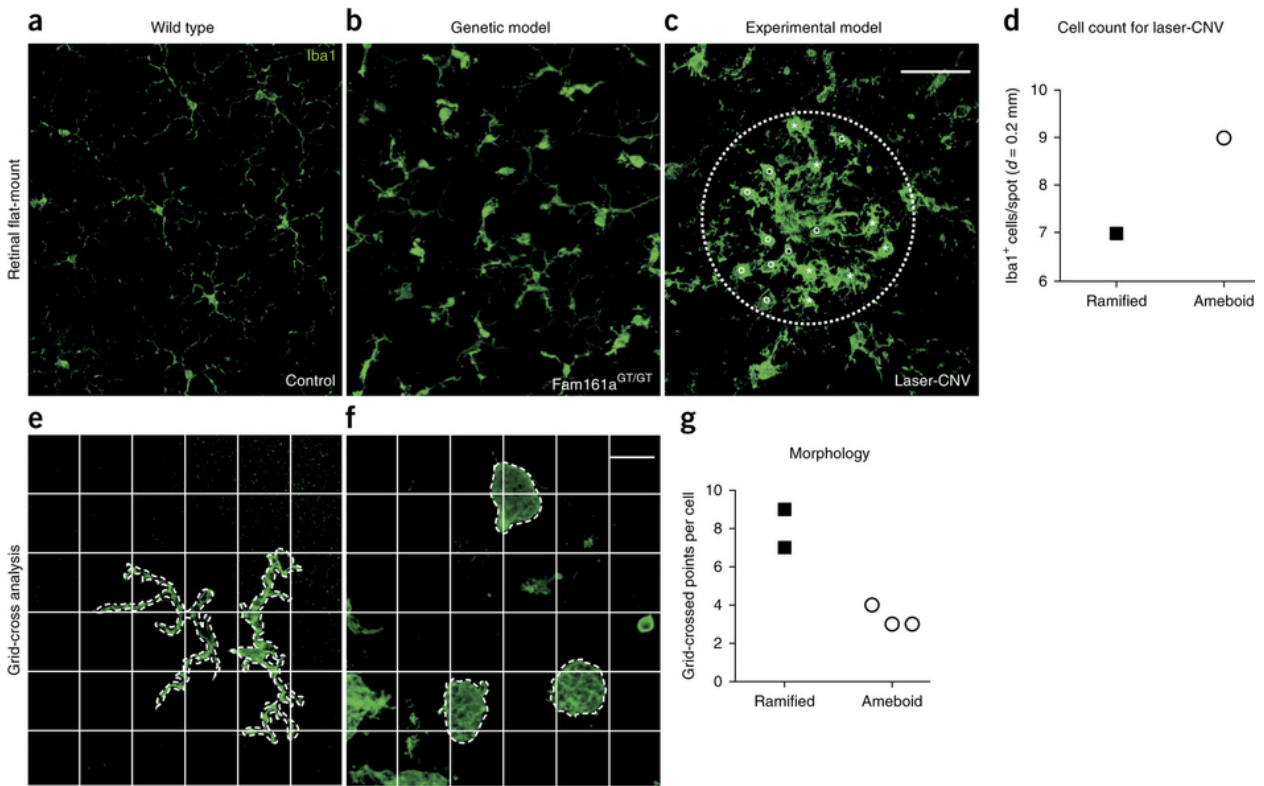


Figure 4: Immunohistochemical analyses of microglia in retinal flat mounts.



**Figure 5:** Flow cytometry analysis of retinal microglia from control mice and animals after light damage.

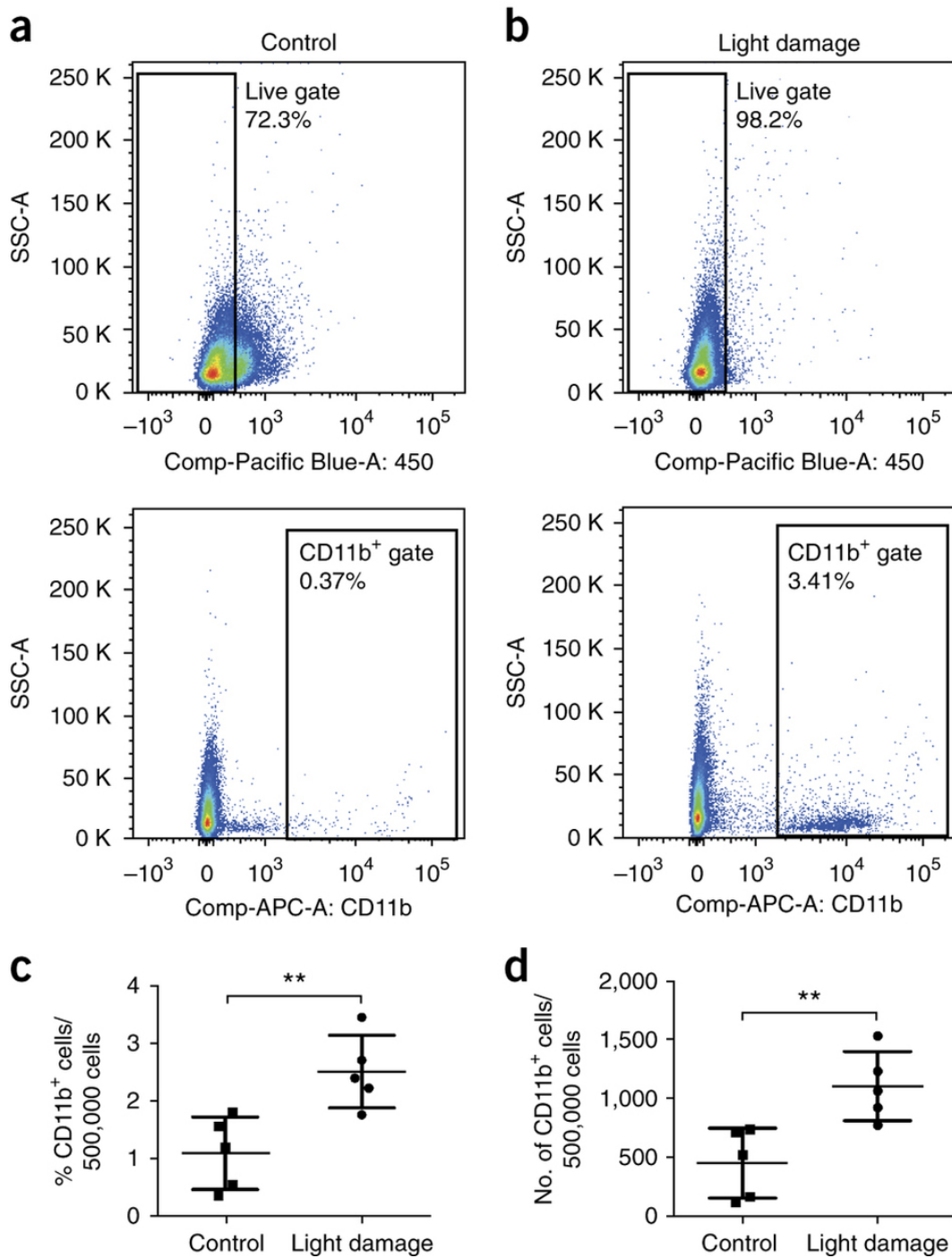


Figure 6: Real-time RT-PCR analyses of representative microglia activation marker genes.

